HHS Public Access

Author manuscript

Radiology. Author manuscript; available in PMC 2016 May 01.

Published in final edited form as:

Radiology. 2016 May ; 279(2): 513–522. doi:10.1148/radiol.2015150947.

Tracking and therapeutic value of human adipose derived mesenchymal stem cell transplantation in reducing venous neointimal hyperplasia associated with arteriovenous fistula

Binxia Yang, MD, PhD[1,*], **Akshaar Brahmbhatt, BS**[1,*], **Evelyn NievesTorres, PhD**[1,*], **Brian Thielen**[1], **Deborah L. McCall, MS**[1], **Sean Engel**[1], **Aditya Bansal, PhD**[1], **Mukesh K. Pandey, PhD**[1], **Allan B. Dietz, PhD**, **Edward B. Leof, PhD**[2], **Timothy R. DeGrado, PhD**[1], **Debabrata Mukhopadhyay, PhD**[2], and **Sanjay Misra, MD**[1,2]

[1]Vascular and Interventional Radiology Translational Laboratory, Department of Radiology, Mayo Clinic, Rochester, Minnesota, USA

[2]Department of Biochemistry and Molecular Biology, Mayo Clinic, Rochester, Minnesota, USA

Abstract

Purpose—The purpose of this study was to determine if adventitial transplantation of human adipose derived mesenchymal stem cell (MSC) to the outflow vein of B6.Cg-*Foxn1*^{nu}/J mice with AVF at the time of creation would reduce monocyte chemoattractant protein-1 (*Mcp-1*) gene expression and venous neointimal hyperplasia (VNH). The second aim was to track transplanted ^{89} zirconium (^{89}Zr) labeled MSCs serially by positron emission tomography (PET) imaging for 21 days.

Materials and Methods—All animal experiments were performed according to protocols approved by our institutional animal care and use committee. We used fifty B6.Cg-*Foxn1*^{nu}/J mice to accomplish the aims outlined in the current paper. 2.5×10^5 MSC cells were stably labeled with green fluorescent protein (GFP) and injected into the adventitia of the outflow vein at the time of AVF creation in MSC group. Eleven mice died after AVF placement. Animals were sacrificed at day 7 following AVF placement for real time polymerase chain reaction (qRT-PCR, n=6 for MSC and control groups) and histomorphometric analyses (n=6, n=6 for MSC and control groups) and at day 21 for histomorphometric analysis only (n=6 for MSC and control groups). In a separate group of experiments (n=3), transplanted ^{89}zirconium (^{89}Zr) labeled MSCs animals were serially imaged by PET imaging for 3 weeks. Multiple comparisons were performed with two-way ANOVA followed by Student *t*-test with post hoc Bonferroni's correction.

Results—We observed that in MSC transplanted vessels when compared to control vessels, there was a significant decrease in the *Mcp-1* gene expression (day 7: average reduction: 62%, P=0.029) with a significant increase in the average lumen vessel area (day 7: average increase: 176%, P=0.013; day 21: average increase: 415%, P=0.011); Moreover, this was accompanied with a significant decrease in Ki-67 index (proliferation, day 7: average reduction: 81%, P=0.0003; day

Address correspondence to: Sanjay Misra, MD, FSIR, FAHA, Department of Radiology, Mayo Clinic, 200 First Street SW, Rochester, MN 55905, Telephone: 507-293-3793, Fax: 507-255-7872, misra.sanjay@mayo.edu.

Disclosures: The authors have none.

21: average reduction: 60%, P=0.016 Prolonged retention of MSCs at the adventitia was evidenced by serial PET images of ^{89}Zr-labeled cells.

Conclusion—These results indicate that adventitial transplantation of MSC decreases *Mcp-1* gene expression accompanied with a reduction in VNH.

Introduction

In the United States, more than 570,000 patients have end-stage renal disease (ESRD) and the majority of the patients require hemodialysis for the purification of their blood (1). An optimally functioning hemodialysis vascular access is required so that patients may undergo purification of their blood and removal of electrolytes. The preferred hemodialysis vascular access is the arteriovenous fistula (AVF) and less than two-thirds of the patients have a well functioning AVF at one year. The majority of AVF will fail because of venous neointimal hyperplasia (VNH) and venous stenosis formation (2, 3).

There are many factors which are thought to contribute to the formation of VNH including hypoxia, shear stress, oxidative stress, and inflammation (4). It is hypothesized that these factors result in elaboration of pro-inflammatory cytokines including monocyte chemoattractant protein-1 (MCP-1) and others (5–7). As a consequence, this leads to accumulation of macrophages, leukocytes, and smooth muscle cells as identified by histologic analysis of specimens removed from the venous stenosis (8).

Mesenchymal stem cells (MSCs) have been isolated and expanded from several different sources including the bone marrow, adipose tissue, and cord blood (9). These cells have anti-inflammatory properties that can result in homeostasis, repair, and regeneration in pathologic responses caused by vascular injury (10). Other studies have demonstrated that MSC transplantation can reduce fibrosis in the heart, lung, liver, and kidney in experimental animal models (11–16). Along with anti-inflammatory properties, studies have demonstrated that MSCs can inhibit the proliferative effects of monocytes, tumor cells, and cardiac fibroblasts (17–20). Finally, MSCs have been shown to reduce hypoxic injury after myocardial infarction because they home to regions of hypoxia (21, 22). In animal models of AVF or graft failure and in clinical specimens, increased expression levels of hypoxia inducible factor-1 alpha (HIF-1α) have been observed. Because of these multiple different properties, MSCs have generated interest for their potential application for alleviating vascular injury. We used adipose derived MSCs from humans that have been manufactured with good manufacturing practice and are currently being used in several clinical trials at our institution.

Taken collectively, we hypothesized that adventitial transplantation of MSCs to the outflow vein of the AVF at the time of creation would reduce pro-inflammatory cytokines including *Mcp-1* and thereby reducing VNH formation (23, 24). The purpose of this study was to determine if adventitial transplantation of human adipose derived mesenchymal stem cell (MSC) to the outflow vein of B6.Cg-*Foxn1*^{nu}/J mice with AVF at the time of creation would reduce monocyte chemoattractant protein-1 (*Mcp-1*) gene expression and venous neointimal hyperplasia (VNH). The second aim was to track transplanted ^{89} zirconium (^{89}Zr) labeled MSCs serially by positron emission tomography (PET) imaging for 21 days.

Materials and Methods

AD is inventor of technology and has a leadership position within the company that supplies technology for growing MSCs used in the paper. He did not have access to the data. TD has a patent pending on Zr-89 labeling of cells. SM and AD have a patent pending on using MSCs for preventing stenosis formation in hemodialysis vascular accesses. The data were under the control of BY, AB, ENT, DLM, SE, AB, MKP, TRD, and SM. They were analyzed by BY, AB, ENT, DLM, SE, AB, MKP, TRD, and SM.

Experimental animals

All animal experiments were performed according to protocols approved by our institutional animal care and use committee. Housing and handling of the animals was performed in accordance with the Public Health Service Policy on Humane Care and Use of Laboratory Animals, which was revised in 2000. Animals were housed at 22° C temperature, 41% relative humidity, and 12-/12-h light/dark cycles. Animals were allowed access to water and food ad libitum. Fifty B6.Cg-*Foxn1*^{nu}/J mice weighting 20–25-g and ages approximately 6–8 weeks were purchased from the Charles River Laboratories (Wilmington, MA). These animals lack a thymus, are unable to produce T cells, and are therefore immunodeficient which is ideal for xenograft research. Anesthesia was achieved with intraperitoneal injection of a mixture of ketamine hydrochloride (0.1–0.2 mg/g) and xylazine (0.02 mg/g). Arteriovenous fistula (AVF) between right carotid artery to the ipsilateral jugular vein was created as described previously (25). 2.5×10^5 MSC cells stably labeled with green fluorescent protein (GFP) in 5-uL of media were injected into the adventitia of the outflow vein at the time of AVF creation in MSC group. 2×10^5 MSCs labeled with GFP were injected into the adventitia of the outflow vein at the time of AVF creation (Fig. S1). Eleven mice died after cell transplantation. Animals were sacrificed at day 7 for either histomorphometric or qRT-PCR analyses for each of the following groups: AVF only (**C**, n=6) and MSC (**M**, n=6). Another group of animals were sacrificed at day 21 after fistula placement for histomorphometric and immuno-histochemical analyses for the following groups: AVF only (**C**, n=6) and **M** (n=6, Fig. S2). In a separate group of experiments, 3 mice were used for tracking Zr^{89} labeled MSCs and 3 mice had free Zr^{89} administered to the adventitia of the outflow vein after creation of an AVF.

Human MSCs preparation

Human MSCs from healthy donors were obtained from the Human Cellular Therapy Laboratory. These cells have been characterized with respect to surface markers and described elsewhere (26). Briefly, they are they are CD73 (+), CD90 (+), CD105 (+), CD44 (+) and HLA-ABC (+) are being used in several clinical trials.

GFP transfection

MSCs were transfected with GFP lentivirus from Dr. Ikeda’s laboratory. MSCs were grown in media containing the GFP lentivirus overnight. The media was changed to complete growth media the next day and cells were checked for fluorescence after 48 hours. Once

fluorescence was confirmed, the cells were cultured in complete media containing 1ug/mL puromycin. Cells containing the plasmid were expanded in complete growth media.

^{89}Zr-desferrioxamine-NCS (^{89}Zr-DBN) labeling and *in vivo* stem cell tracking

Non-invasive PET imaging was used to evaluate the biodistribution of MSCs delivered to the adventitia outside the AVF in CD1-*Foxn1nu* mice. For this, the MSCs were labeled with a biostable radiolabel ^{89}Zr-desferrioxamine (DBN) as previously described [REF 1]. The 3.3 d half-life of ^{89}Zr allowed for assessment of localization of delivered MSCs over 3 weeks post-delivery. The ^{89}Zr-DBN based radiolabeling is well tolerated by cells with no loss of viability or efflux of radiolabel (27). Following delivery of 2×10^5 ^{89}Zr-labeled MSCs (at radioactivity concentration of ~ 0.55 MBq/10^6 cells) into the adventitia, the ^{89}Zr-labeled MSCs were tracked for 3 weeks using a small animal PET/X-ray system (Sofie BioSystems Genesys4, Culver City, CA, USA). In the control group, $^{89}Zr(HPO_4)_2$ (0.28 MBq) was delivered into the adventitia. PET images were normalized to units of Standardized Uptake Value (SUV) = tissue radioactivity concentration / (injected dose / body wt. (g)).

Immunohistochemistry and morphometric analysis

After fixation with formalin and processing, the samples were embedded in paraffin. Histological sectioning began at the outflow vein segment. Routinely, 80 to 120, 5-um sections were obtained and the cuff used to make the anastomosis could be visualized. Every 25-μm, 2–4 sections were stained with Hematoxylin and eosin, Ki-67, α-SMA, HIF-1α, CD68, FSP-1, or TUNEL performed on paraffin-embedded sections from the outflow vein. Using the EnVision (DAKO, Carpinteria, CA) method with a heat-induced antigen retrieval step (28). The following antibodies were used: mouse monoclonal antibody Ki-67 (DAKO, 1:400) or rabbit polyclonal antibody to mouse for CD68, α-SMA, FSP-1, and HIF-1α (Abcam, 1:600) IgG antibody staining was performed to serve as controls. Sections immunostained for Hematoxylin and eosin, Ki-67, α-SMA, HIF-1α, CD68, FSP-1, or TUNEL were viewed using an Axioplan 2 Microscope (Zeiss, Oberkochen, Germany) equipped with a Neo-Fluor × 20/0.50 objective and digitized to capture a minimum of 1030 × 1300 pixels using a Axiocam camera (Zeiss). Images were obtained which included the entire cross section of the venous anastomosis using KS 400 Image Analysis software (Zeiss). Ki-67, HIF-1α, or TUNEL-positive (brown) and total nuclei (brown + blue) were highlighted, in turn, by selecting the appropriate RGB (red-green-blue) color intensity range and then counted. The color intensity was adjusted for each section to account for decreasing intensity of positive staining over time. The Ki-67, HIF-1α, or TUNEL indices (positive cells/total cells × 100) were calculated for each section. This was repeated twice to ensure intraobserver variability was less than 10%. The area of the neointima and media + adventitia for the venous anastomosis was determined by manually tracing the different layers of the vessel wall following immunostaining with Hematoxylin and eosin. The neointima was defined as the area above the internal elastic lamina, which was easily determined from the media for 3 to 5 sections. The media + adventitia area was defined from the internal elastic lamina to the fat surrounding the vessel wall.

TdT-mediated dNTP nick end labeling (TUNEL) staining

TdT-mediated dNTP nick end labeling (TUNEL) staining was performed on paraffin-embedded sections from the outflow vein of MSC with scaffold, MSC and Scaffold treated vessels as specified by the manufacturer (DeadEnd Colorimetric tunnel assay system, G7360, Promega). Negative control is shown where the recombinant terminal deoxynucleotidyl transferase enzyme was omitted.

RNA isolation

The outflow vein was isolated and stored in RNA stabilizing reagent (Qiagen, Gaithersburg, MD) as per the manufactures guidelines. To isolate the RNA, the specimens were homogenized and total RNA from the samples was isolated using RNeasy mini kit (Qiagen) (25).

Real time polymerase chain reaction (qRT-PCR) analysis

Studies have demonstrated that MSCs exert their anti-inflammatory effect through a reduction in gene expression of *Mcp-1* (31). We assessed the gene expression of *Mcp-1* by performing qRT-PCR analysis at day 7 after **M** transplanted vessels when compared to control AVFs alone. Expression for the gene of interest was determined using qRT-PCR analysis as described previously (25). Primers used are shown in table 1.

Statistical methods

Data are expressed as mean ± standard error of the mean (SEM). Multiple comparisons were performed with two-way ANOVA followed by Student *t*-test with post hoc Bonferroni's correction. Significant difference from control value was indicated by $*P<0.05$, $**P<0.01$, $^{\#}P<0.001$, or $^{\#\#}P<0.0001$. JMP version 9 (SAS Institute Inc., Cary, N.C.) was used for statistical analyses.

Results

Localization of MSCs after Adventitial delivery of to the outflow vein of AVF

MSCs were stably transfected with GFP so they could be identified after adventitial delivery using confocal microscopy of the outflow vein performed at different times. This demonstrated that GFP positive cells from the **M** transplanted vessels (blue positive cells, Fig. 1A, **arrow head**) were present at day 7. However, by day 21, there was no visualization of the GFP signal (**data not shown**).

PET images of mice after adventitial delivery of ^{89}Zr-labeled MSCs showed >90% of administered ^{89}Zr-radioactivity retained at the delivery site at day 4 (Figure 1). Adventitial retention of ^{89}Zr-radioactivity cleared slowly from day 4 to day 21, losing ~20% over this period (Fig. 1B). The majority of ^{89}Zr-radioactivity that was cleared from the adventitia appeared to translocate to bones. This result confirmed the results obtained using confocal microscopy with GFP labeled cells at day 7. PET imaging of ^{89}Zr-labeled MSCs allowed tracking of cells beyond 7 days, which was not possible with GFP labeled cells. The retention of a majority of delivered stem cells at the delivery site at day 21 demonstrates that their effect is longer than what was visualized using GFP labeling. In the case of the control

group administered $^{89}Zr(HPO_4)_2$, a similar biodistribution was seen to that of ^{89}Zr-labeled MSCs with the majority (~80%) of radioactivity retained at the delivery site and the rest redistributing to bones.

Adventitial transplantation of MSC reduces gene expression of *MCP-1* at the outflow vein

The average gene expression of *Mcp-1* at outflow vein of **M** transplanted vessels was significantly lower than the **C** group (average reduction: 62%, P=0.029, Fig. 2).

Adventitial transplantation of MSC to the outflow vein reduces the average neointima area/ media+adventitia area and cell density in the neointima while increasing the average lumen vessel area at days 7 and 21

We determined the average lumen vessel area at day 7 and observed that there was a significant increase in the outflow vein removed from **M** transplanted vessels versus **C** group (average increase: 176%, P=0.013, Fig. S3A) and by day 21, it remained significantly increased in the **M** transplanted vessels when compared to **C** group (average increase: 415%, P=0.011). We next determined the average of the neointima area/media+adventitia area. By day 21, there was a significant decrease in the neointima area/media+adventitia area in the outflow vein removed from the **M** transplanted vessels when compared to the **C** group (average reduction: 77%, P=0.013, Fig. S3B).

By day 7, the average cell density of the neointima in the **M** treated vessels was significantly lower than the **C** group (average reduction: 83%, P=0.0007, Fig. S3C) and by day 21, it remained lower in the **M** transplanted vessels when compared to the **C** group (average reduction: 83%, P<0.0001).

Adventitial transplantation of MSC to the outflow vein increases TUNEL staining

We speculated that the decrease in cell density was also due to an increase in apoptosis (34). Apoptosis was evaluated by using TUNEL staining (Fig. 4 **upper panel**). By day 7, the average density of cells staining positive for TUNEL (brown staining nuclei) at the outflow vein of **M** transplanted vessels was significantly increased compared to the **C** group (average increase: 3061%, P<0.0001) and by day 21, it remained higher in the **M** transplanted vessels compared to the **C** group (average increase: 425%, P<0.0001, Fig. S4A). Therefore, these results demonstrate that **M** transplanted vessels have increased TUNEL activity indicating cellular apoptosis when compared to **C** vessels.

Adventitial transplantation of MSC to the outflow vein reduces cellular proliferation at the outflow vein

Because the cellular density was decreased, we determined if this was associated with a reduction in cellular proliferation that was assessed using Ki-67 staining (brown staining nuclei are positive for Ki-67, Fig. 4 **lower panel**). By seven days after fistula placement, there was a significant reduction in the average Ki-67 index in the **M** transplanted vessels when compared to **C** group (average reduction: 81%, P=0.0003, Fig. S4B). By day 21, it remained significantly lower in the **M** transplanted vessels when compared to **C** vessels (average reduction: 60%, P=0.016).

Adventitial transplantation of MSC to the outflow reduces α-SMA and FSP-1 staining

We assessed smooth muscle deposition using α-smooth muscle cell actin staining (Fig. 5 **upper panel**). By day 21, the average α-SMA staining was significantly lower in the **M** transplanted vessels when compared to **C** group (average reduction: 27%; *P*=0.013, Fig. S5A). Fibroblast specific protein-1 (FSP-1) has been used as a fibroblast marker (Fig. 5 **lower panel**). Previous studies have implicated fibroblast to myofibroblast (α-SMA) differentiation resulting in VNH (28, 35). By day 7, we observed a significant decrease in the average FSP-1 staining in the **M** transplanted vessels when compared to **C** group (average reduction: 65%, *P*=0.0003, Fig. S5B). By day 21, it remained significantly lower in the **M** transplanted vessels when compared to **C** group (average reduction: 42% *P*=0.0016). Overall these results indicate that at day 7 there is a reduction in FSP-1 staining followed by a decrease in α-SMA staining by day 21 in **M** transplanted vessels when compared to **C** vessels.

Adventitial transplantation of MSC to the outflow is associated with a reduction in HIF-1α staining

We quantified HIF-1α staining to assess whether MSC transplantation had an effect on the expression of HIF-1α at the outflow vein of AVF. Brown staining nuclei are positive for HIF-1α (Fig. 6 **upper panel**). By day 7, there was significant reduction in the average density of HIF-1α staining **M** transplanted vessels when compared to **C** vessels (average reduction: 67%, *P*<0.0001, Fig. S6A). By day 21, it remained significantly lower in the **M** treated vessels when compared to **C** vessels (average reduction: 62%, *P*=0.0005). Overall these results indicate that there is decreased expression in HIF-1α in **M** transplanted vessels when compared to **C** treated vessels.

Adventitial transplantation of MSC to the outflow is associated with a reduction in CD68 staining

Cells staining brown in the cytoplasm are positive for CD68 (Fig. 6 **lower panel**). By day 7, there was significant reduction in the average density of CD68 staining in the **M** treated vessels when compared to **C** vessels (average reduction: 51%, *P*=0.033, Fig. S6B). Overall, there is a significant decrease in CD68 staining in the **M** transplanted vessels when compared to controls.

Discussion

In our study, we demonstrate that adventitial transplantation of human adipose derived MSCs to the outflow vein of AVF in a murine model reduces venous neointimal hyperplasia. This is mediated by a significant decrease in the gene expression of *Mcp-1* in the outflow vein transplanted with MSCs compared to controls at day 7. There is a significant increase in average TUNEL staining with a decrease in proliferation. In addition, there is a significant decrease in the FSP-1, CD68, and α-SMA staining accompanied with a decrease in average HIF-1α staining. Finally, Zr89 labeled MSCs can be tracked up to 3-weeks after adventitial delivery.

Previous studies have shown that there is increased gene expression of *Mcp-1* at the AVF (5–7). Genetic deletion of Mcp-1 in experimental animal models of AVF failure was associated with a reduction in venous stenosis formation (5). Mcp-1 was localized to the endothelium, smooth muscle cells, and leukocytes. In the present study, we observed that MSC transplanted vessels had reduced expression of Mcp-1 accompanied with a reduction in cells staining positive for FSP-1, α-SMA, and CD68. Adventitial transplantation of MSC to the outflow vein at the time of AVF results in a reduction of several pro-inflammatory genes including *Mcp-1*. Our findings are consistent with the previous studies which have demonstrated that human MSC transplantation can reduce *Mcp-1* gene expression in experimental animal models of focal cerebral ischemia (37). Increased expression of the MCP-1/CCL2 axis is associated with the pathogenesis of several different fibrotic models involving the lung, kidney, and liver (38–41). Notably, *Mcp-1* is implicated in dysfunction of AVF clinically and in experimental animal models (5, 42). Studies conducted in patients with hemodialysis have shown that there are increased serum levels of MCP-1 and this is considered to be a risk factor for AVF dysfunction (43, 44).

Venous neointimal hyperplasia is characterized by an increase in cellular proliferation, extra extracellular matrix deposition and a decrease in apoptosis (8, 33, 45). Previous studies have demonstrated inhibitory effects of MSC on proliferation of target cells such as monocytes, tumor cells, and cardiac fibroblasts (17–20). Conversely, MSC have been shown to induce proliferation and migration in lung fibroblasts and endothelial cells (46, 47). Studies conducted by our laboratories and others have demonstrated that adventitial and medial fibroblasts can convert to myofibroblasts [α-SMA (+)] that can proliferate and migrate leading to VNH formation (35, 48).

In our study, we assessed cellular proliferation by performing Ki-67 staining and observed a significant reduction in cellular proliferation in transplanted vessels removed from animals treated with MSC when compared to controls. MSCs can exert anti-proliferative effect mediated in part by decreasing *Mcp-1* expression. Our finding is consistent with a study conducted *in vitro* in which CD14+ cells isolated from peripheral blood enhanced fibroblast proliferation mediated through MCP-1 (49). In addition to reduced cellular proliferation, we also observed a significant decrease in cellular density accompanied with a significant increase in TUNEL staining.

Hypoxic injury to the vessel wall of the outflow vein at the time of AVF placement and arterial bypass grafts can result in venous neointimal hyperplasia (50–52). Several studies have demonstrated increased HIF-1α expression in animal models of hemodialysis graft failure and in clinical specimens from patients with hemodialysis vascular access failure (23, 36). In our study, we found that adventitial transplantation of MSC to adventitia of the outflow vein in a murine model results in a significant reduction in the expression of HIF-1α. These findings indicate that MSC transplantation to the adventitia of outflow vein is associated with a reduction in expression of HIF-1α therefore possibly reducing hypoxia-induced inflammatory response in the vessel wall. It is well known that macrophages can home to areas of vascular injury associated with hypoxia, and we hypothesize that the reduction in HIF-1α and thus hypoxia is responsible for the decreased CD68 staining.

PET imaging of ^{89}Zr-labeled MSCs showed the majority (~80%) of the radiolabel to be retained at the adventitial delivery site, even out to 3 weeks post-delivery. This result confirms that the cells are in contact with the adventitia of the outflow vein for a prolonged period post-delivery. The similar imaging findings with $^{89}Zr(HPO_4)_2$, which delivered ^{89}Zr in its “free” cationic form to the adventitia, would appear to indicate that the adventitia is not well perfused. Thus, the slow release of ^{89}Zr-labeled MSCs from the adventitia cannot be interpreted as strong evidence of specific binding of the cells to the adventitia. In contrast, ^{89}Zr-labeled MSCs delivered intravenously home to lung, followed by liver and bones and free $^{89}Zr(HPO_4)_2$ is mainly localized in liver and bones. These differences in biodistribution provide further evidence that the prolonged retention of both ^{89}Zr-labeled MSCs and $^{89}Zr(HPO_4)_2$ may be explained by the lack of perfusion on the surface of the adventitia due to a less defined vasa vasorum surrounding the vein when compared to the artery (29). In addition, the use of ^{89}Zr-labeled MSCs was more sensitive for detecting cellular location after delivery than GFP labeling.

There are several limitations to our study. We used an immunodeficient mouse and potential T cell mediated mechanism involved in pathophysiology of VNH could not be evaluated. A murine model of normal kidney function was employed and thus the effects of chronic kidney disease could not be evaluated. Finally, these results need to be corroborated using larger animal models as the murine model may not simulate the clinical scenario.

Practical applications

In conclusion, we demonstrate that adventitial transplantation of human adipose derived MSCs to the outflow vein of a murine model of AVF results in a decrease in the gene expression of *Mcp-1*. This resulted in a reduction in venous neointimal hyperplasia accompanied with a decrease in cell proliferation and an increase in apoptosis with positive vascular remodeling. The clinical importance of this study is that it provides rationale for using MSC transplantation in patients with hemodialysis AVF access for reducing VNH and highlights that MSCs can be tracked after delivery using PET imaging of ^{89}Zr-labeled MSCs.

Supplementary Material

Refer to Web version on PubMed Central for supplementary material.

Acknowledgments

AB has received a Howard Hughes Medical Institute grant. This work was funded by a HL098967 (SM) from the National Heart, Lung, And Blood Institute. The authors would like to thank Dr. Jay Mandrekar for his biostatistical expertise in interpreting the results.

References

1. Collins AJ, Foley RN, Chavers B, et al. US Renal Data System 2013 Annual Data Report. American journal of kidney diseases: the official journal of the National Kidney Foundation. 2014; 63(1 Suppl):A7. [PubMed: 24360288]
2. Roy-Chaudhury P, Kelly BS, Zhang J, et al. Hemodialysis vascular access dysfunction: from pathophysiology to novel therapies. Blood purification. 2003; 21(1):99–110. [PubMed: 12596755]

3. Rotmans JI, Pasterkamp G, Verhagen HJ, Pattynama PM, Blankestijn PJ, Stroes ES. Hemodialysis access graft failure: time to revisit an unmet clinical need? Journal of nephrology. 2005; 18(1):9–20. [PubMed: 15772918]
4. Riella MC, Roy-Chaudhury P. Vascular access in haemodialysis: strengthening the Achilles' heel. Nature reviews Nephrology. 2013; 9(6):348–57. [PubMed: 23591442]
5. Juncos JP, Grande JP, Kang L, et al. MCP-1 contributes to arteriovenous fistula failure. Journal of the American Society of Nephrology: JASN. 2011; 22(1):43–8. [PubMed: 21115617]
6. Mattana J, Effiong C, Kapasi A, Singhal PC. Leukocyte-polytetrafluoroethylene interaction enhances proliferation of vascular smooth muscle cells via tumor necrosis factor-alpha secretion. Kidney international. 1997; 52(6):1478–85. [PubMed: 9407493]
7. Dukkipati R, Molnar MZ, Park J, et al. Association of Vascular Access Type with Inflammatory Marker Levels in Maintenance Hemodialysis Patients. Seminars in dialysis. 2013
8. Roy-Chaudhury P, Kelly BS, Miller MA, et al. Venous neointimal hyperplasia in polytetrafluoroethylene dialysis grafts. Kidney international. 2001; 59(6):2325–34. [PubMed: 11380837]
9. Pittenger MF, Mackay AM, Beck SC, et al. Multilineage potential of adult human mesenchymal stem cells. Science. 1999; 284(5411):143–7. [PubMed: 10102814]
10. Prockop DJ, Olson SD. Clinical trials with adult stem/progenitor cells for tissue repair: let's not overlook some essential precautions. Blood. 2007; 109(8):3147–51. [PubMed: 17170129]
11. Oyagi S, Hirose M, Kojima M, et al. Therapeutic effect of transplanting HGF-treated bone marrow mesenchymal cells into CCl4-injured rats. Journal of hepatology. 2006; 44(4):742–8. [PubMed: 16469408]
12. Abdel Aziz MT, Atta HM, Mahfouz S, et al. Therapeutic potential of bone marrow-derived mesenchymal stem cells on experimental liver fibrosis. Clinical biochemistry. 2007; 40(12):893–9. [PubMed: 17543295]
13. Nagaya N, Kangawa K, Itoh T, et al. Transplantation of mesenchymal stem cells improves cardiac function in a rat model of dilated cardiomyopathy. Circulation. 2005; 112(8):1128–35. [PubMed: 16103243]
14. Ortiz LA, Gambelli F, McBride C, et al. Mesenchymal stem cell engraftment in lung is enhanced in response to bleomycin exposure and ameliorates its fibrotic effects. Proceedings of the National Academy of Sciences of the United States of America. 2003; 100(14):8407–11. [PubMed: 12815096]
15. Ninichuk V, Gross O, Segerer S, et al. Multipotent mesenchymal stem cells reduce interstitial fibrosis but do not delay progression of chronic kidney disease in collagen4A3-deficient mice. Kidney international. 2006; 70(1):121–9. [PubMed: 16723981]
16. Caplan AI. Why are MSCs therapeutic? New data: new insight. The Journal of pathology. 2009; 217(2):318–24. [PubMed: 19023885]
17. Ramasamy R, Fazekasova H, Lam EW, Soeiro I, Lombardi G, Dazzi F. Mesenchymal stem cells inhibit dendritic cell differentiation and function by preventing entry into the cell cycle. Transplantation. 2007; 83(1):71–6. [PubMed: 17220794]
18. Ramasamy R, Lam EW, Soeiro I, Tisato V, Bonnet D, Dazzi F. Mesenchymal stem cells inhibit proliferation and apoptosis of tumor cells: impact on in vivo tumor growth. Leukemia. 2007; 21(2):304–10. [PubMed: 17170725]
19. Li L, Zhang S, Zhang Y, Yu B, Xu Y, Guan Z. Paracrine action mediate the antifibrotic effect of transplanted mesenchymal stem cells in a rat model of global heart failure. Molecular biology reports. 2009; 36(4):725–31. [PubMed: 18368514]
20. Ohnishi S, Sumiyoshi H, Kitamura S, Nagaya N. Mesenchymal stem cells attenuate cardiac fibroblast proliferation and collagen synthesis through paracrine actions. FEBS letters. 2007; 581(21):3961–6. [PubMed: 17662720]
21. Das R, Jahr H, van Osch GJ, Farrell E. The role of hypoxia in bone marrow-derived mesenchymal stem cells: considerations for regenerative medicine approaches. Tissue engineering Part B, Reviews. 2010; 16(2):159–68. [PubMed: 19698058]

22. Hu X, Yu SP, Fraser JL, et al. Transplantation of hypoxia-preconditioned mesenchymal stem cells improves infarcted heart function via enhanced survival of implanted cells and angiogenesis. The Journal of thoracic and cardiovascular surgery. 2008; 135(4):799–808. [PubMed: 18374759]

23. Misra S, Shergill U, Yang B, Janardhanan R, Misra KD. Increased expression of HIF-1alpha, VEGF-A and its receptors, MMP-2, TIMP-1, and ADAMTS-1 at the venous stenosis of arteriovenous fistula in a mouse model with renal insufficiency. J Vasc Interv Radiol. 2010; 21(8): 1255–61. [PubMed: 20598569]

24. Das M, Burns N, Wilson SJ, Zawada WM, Stenmark KR. Hypoxia exposure induces the emergence of fibroblasts lacking replication repressor signals of PKCzeta in the pulmonary artery adventitia. Cardiovascular research. 2008; 78(3):440–8. [PubMed: 18218684]

25. Yang B, Shergill U, Fu AA, Knudsen B, Misra S. The mouse arteriovenous fistula model. J Vasc Interv Radiol. 2009; 20(7):946–50. [PubMed: 19555889]

26. Crespo-Diaz R, Behfar A, Butler GW, et al. Platelet lysate consisting of a natural repair proteome supports human mesenchymal stem cell proliferation and chromosomal stability. Cell Transplant. 2011; 20(6):797–811. [PubMed: 21092406]

27. Bansal A, Pandey MK, Demirhan YE, et al. Novel 89Zr cell labeling approach for PET-based cell trafficking studies. EJNMMI Research. 2015; 5:19. [PubMed: 25918673]

28. Misra S, Doherty MG, Woodrum D, et al. Adventitial remodeling with increased matrix metalloproteinase-2 activity in a porcine arteriovenous polytetrafluoroethylene grafts. Kidney international. 2005; 68(6):2890–900. [PubMed: 16316367]

29. Yang B, Janardhanan R, Vohra P, et al. Adventitial transduction of lentivirus-shRNA-VEGF-A in arteriovenous fistula reduces venous stenosis formation. Kidney international. 2014 Feb; 85(2): 289–306. [PubMed: 23924957]

30. Janardhanan R, Yang B, Vohra P, et al. Simvastatin reduces venous stenosis formation in a murine hemodialysis vascular access model. Kidney international. 2013 Aug; 84(2):338–52. [PubMed: 23636169]

31. Wise AF, Williams TM, Kiewiet MB, et al. Human mesenchymal stem cells alter macrophage phenotype and promote regeneration via homing to the kidney following ischemia-reperfusion injury. American journal of physiology Renal physiology. 2014; 306(10):F1222–35. [PubMed: 24623144]

32. Rekhter M, Nicholls S, Ferguson M, Gordon D. Cell proliferation in human arteriovenous fistulas used for hemodialysis. Arterioscler Thromb. 1993; 13(4):609–17. [PubMed: 8096766]

33. Swedberg SH, Brown BG, Sigley R, Wight TN, Gordon D, Nicholls SC. Intimal fibromuscular hyperplasia at the venous anastomosis of PTFE grafts in hemodialysis patients. Clinical, immunocytochemical, light and electron microscopic assessment. Circulation. 1989; 80(6):1726–36. [PubMed: 2688974]

34. Shay-Salit A, Shushy M, Wolfovitz E, et al. VEGF receptor 2 and the adherens junction as a mechanical transducer in vascular endothelial cells. Proc Natl Acad Sci U S A. 2002; 99(14): 9462–7. [PubMed: 12080144]

35. Wang Y, Krishnamoorthy M, Banerjee R, et al. Venous stenosis in a pig arteriovenous fistula model--anatomy, mechanisms and cellular phenotypes. Nephrology, dialysis, transplantation: official publication of the European Dialysis and Transplant Association - European Renal Association. 2008; 23(2):525–33.

36. Misra S, Fu AA, Rajan DK, et al. Expression of hypoxia inducible factor-1 alpha, macrophage migration inhibition factor, matrix metalloproteinase-2 and -9, and their inhibitors in hemodialysis grafts and arteriovenous fistulas. J Vasc Interv Radiol. 2008; 19(2 Pt 1):252–9. [PubMed: 18341958]

37. Wang H, Nagai A, Sheikh AM, et al. Human mesenchymal stem cell transplantation changes proinflammatory gene expression through a nuclear factor-kappaB-dependent pathway in a rat focal cerebral ischemic model. Journal of neuroscience research. 2013; 91(11):1440–9. [PubMed: 23996632]

38. Hartl D, Griese M, Nicolai T, et al. A role for MCP-1/CCR2 in interstitial lung disease in children. Respiratory research. 2005; 6:93. [PubMed: 16095529]

39. Okuma T, Terasaki Y, Kaikita K, et al. C-C chemokine receptor 2 (CCR2) deficiency improves bleomycin-induced pulmonary fibrosis by attenuation of both macrophage infiltration and production of macrophage-derived matrix metalloproteinases. The Journal of pathology. 2004; 204(5):594–604. [PubMed: 15538737]
40. Tesch GH. MCP-1/CCL2: a new diagnostic marker and therapeutic target for progressive renal injury in diabetic nephropathy. American journal of physiology Renal physiology. 2008; 294(4):F697–701. [PubMed: 18272603]
41. Kanno K, Tazuma S, Nishioka T, Hyogo H, Chayama K. Angiotensin II participates in hepatic inflammation and fibrosis through MCP-1 expression. Digestive diseases and sciences. 2005; 50(5):942–8. [PubMed: 15906773]
42. Liu BC, Li L, Gao M, Wang YL, Yu JR. Microinflammation is involved in the dysfunction of arteriovenous fistula in patients with maintenance hemodialysis. Chinese medical journal. 2008; 121(21):2157–61. [PubMed: 19080177]
43. Papayianni A, Alexopoulos E, Giamalis P, et al. Circulating levels of ICAM-1, VCAM-1, and MCP-1 are increased in haemodialysis patients: association with inflammation, dyslipidaemia, and vascular events. Nephrology, dialysis, transplantation: official publication of the European Dialysis and Transplant Association - European Renal Association. 2002; 17(3):435–41.
44. De Marchi S, Falleti E, Giacomello R, et al. Risk factors for vascular disease and arteriovenous fistula dysfunction in hemodialysis patients. Journal of the American Society of Nephrology: JASN. 1996; 7(8):1169–77. [PubMed: 8866409]
45. Rekhter M, Nicholls S, Ferguson M, Gordon D. Cell proliferation in human arteriovenous fistulas used for hemodialysis. Arteriosclerosis and thrombosis: a journal of vascular biology / American Heart Association. 1993; 13(4):609–17. [PubMed: 8096766]
46. Salazar KD, Lankford SM, Brody AR. Mesenchymal stem cells produce Wnt isoforms and TGF-beta1 that mediate proliferation and procollagen expression by lung fibroblasts. American journal of physiology Lung cellular and molecular physiology. 2009; 297(5):L1002–11. [PubMed: 19734317]
47. Potapova IA, Gaudette GR, Brink PR, et al. Mesenchymal stem cells support migration, extracellular matrix invasion, proliferation, and survival of endothelial cells in vitro. Stem Cells. 2007; 25(7):1761–8. [PubMed: 17395769]
48. Li L, Terry CM, Blumenthal DK, et al. Cellular and morphological changes during neointimal hyperplasia development in a porcine arteriovenous graft model. Nephrol Dial Transplant. 2007; 22(11):3139–46. [PubMed: 17602194]
49. Liao WT, Yu HS, Arbiser JL, et al. Enhanced MCP-1 release by keloid CD14+ cells augments fibroblast proliferation: role of MCP-1 and Akt pathway in keloids. Experimental dermatology. 2010; 19(8):e142–50. [PubMed: 20100200]
50. Lata C, Green D, Wan J, Roy S, Santilli SM. The role of short-term oxygen administration in the prevention of intimal hyperplasia. Journal of vascular surgery. 2013; 58(2):452–9. [PubMed: 23380177]
51. Lee ES, Bauer GE, Caldwell MP, Santilli SM. Association of artery wall hypoxia and cellular proliferation at a vascular anastomosis. J Surg Res. 2000; 91(1):32–7. [PubMed: 10816346]
52. Santilli SM, Wernsing SE, Lee ES. Transarterial wall oxygen gradients at a prosthetic vascular graft to artery anastomosis in the rabbit. Journal of vascular surgery. 2000; 31(6):1229–39. [PubMed: 10842160]

Advances in Knowledge

- We observed that in mesenchymal stem cells (MSC) transplanted vessels when compared to control vessels, there was a significant decrease in the *Mcp-1* gene expression (day 7: average reduction: 62%, P=0.029) with a significant increase in the average lumen vessel area (day 7: average increase: 176%, P=0.013; day 21: average increase: 415%, P=0.011); significant decrease in the average neointima area/ media + adventitia area (day 21: average reduction: 77%, P=0.013); and neointima cell density (day 7: average reduction: 83%, P=0.0007; day 21: average reduction: 83%, P<0.0001).
- This was accompanied with a significant decrease in Ki-67 index (proliferation, day 7: average reduction: 81%, P=0.0003; day 21: average reduction: 60%, P=0.016), fibroblast (day 7: average reduction: 65%, P=0.0003; average reduction: 42%, P=0.0016; day 21: average reduction: 42%, P=0.0016; average reduction: 42%, P=0.0016), smooth muscle cell (day 21: average reduction: 27%, P=0.013), and macrophage staining (day 7: average reduction: 51%, P=0.033) with a significant increase in cellular apoptosis (day 7: average increase: 3061%, P<0.0001; day 21: average increase: 425%, P<0.0001).
- We were able to track transplanted ^{89}Zr-labeled MSCs by PET imaging for 21-days.

Implication for Patient Care

Adipose derived mesenchymal stem cell transplantation to the adventitia of the outflow vein of arteriovenous fistula (AVF) may potentially help reduce venous stenosis formation.

Author Manuscript

Author Manuscript

Author Manuscript

Summary statement

These results indicate that adventitial transplantation of MSC may be a potential translational therapy for reducing venous stenosis formation.

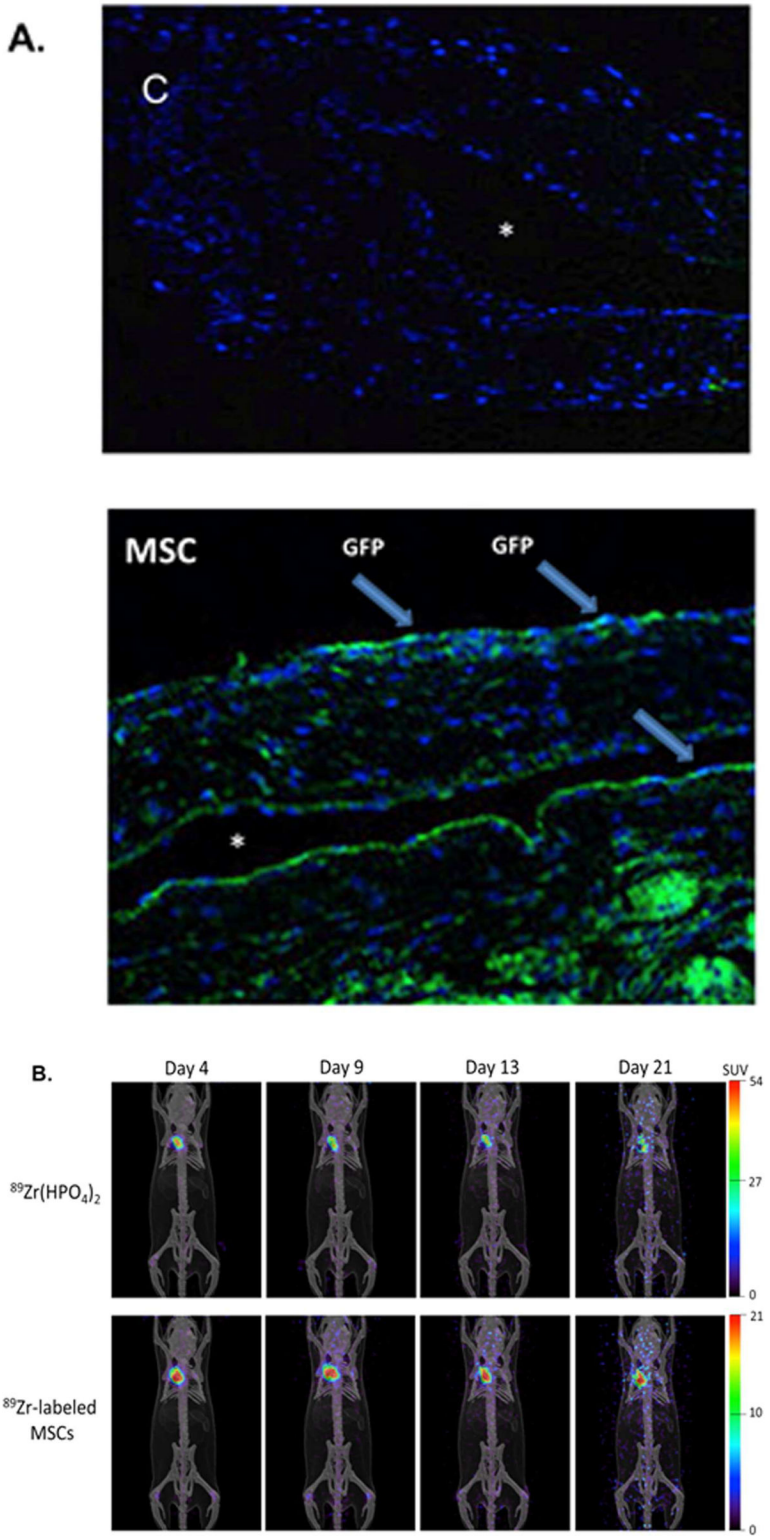

Figure 1.

A. Localization of human adipose derived mesenchymal stem cells (MSCs). 2.5×10^5 MSCs were stable transfected with GFP were injected into the adventitia of the outflow vein of

AVF at the time of creation. GFP labeled human adipose derived mesenchymal stem cells (MSCs) are present at day 7 in MSC transplanted vessels (**M**) compared to outflow vein vessels removed from animals (**C**) after AVF placement. Blue are nuclei. There are GFP positive cells (arrows) in the vessel wall of the outflow vein at day 7. * is lumen. **B**. Serial PET images of ^{89}Zr distribution in mice after adventitial delivery of ^{89}Zr-labeled MSCs or $^{89}Zr(HPO_4)_2$. The anatomical reference skeleton images are formed using the mouse atlas registration system (MARS) algorithm with information obtained from the stationary top-view planar x-ray projector and side-view optical camera.

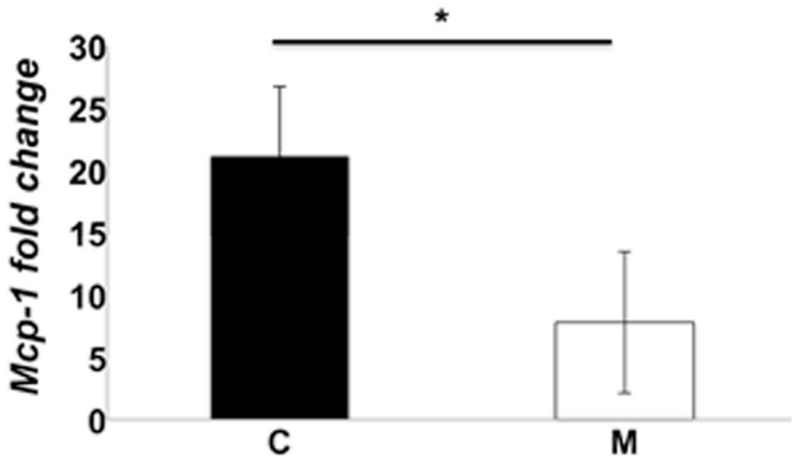

Figure 2.

Monocyte chemoattractant protein-1 (*Mcp-1*) gene expression at day 7 in MSC transplanted vessels (**M**) compared to outflow vein vessels removed from animals (**C**). There is a significant decrease in the mean *Mcp-1* gene expression in the **M** transplanted vessels when compared to **C** group ($P<0.05$). Each bar shows the mean ± SEM of 4–6 animals per group. Two-way ANOVA with Student *t* test was performed. Significant differences among **M** transplanted and **C** vessels is indicated by $*P<0.05$.

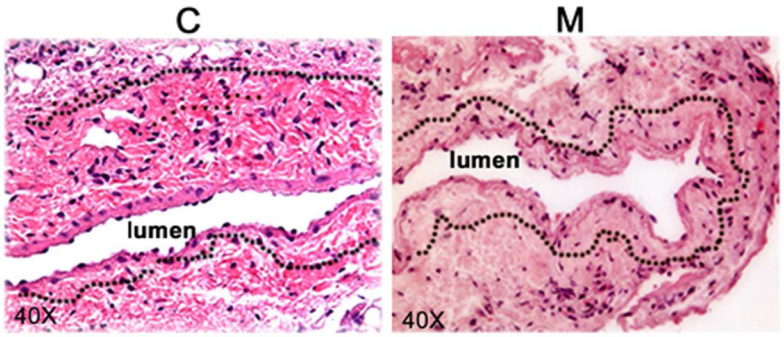

Figure 3.

Hematoxylin and eosin (H and E) staining of mesenchymal stem cell transplanted vessels (**M**) compared to outflow vein vessels removed from animals with AVF only (**C**) at day 7 and 21 after placement. A representative section after Hematoxylin and eosin (H and E) staining in **M** transplanted or **C** vessels at day 7 after AVF placement is shown. Arrow is neointima. All are original magnification X 40. Bar is 50-μM.

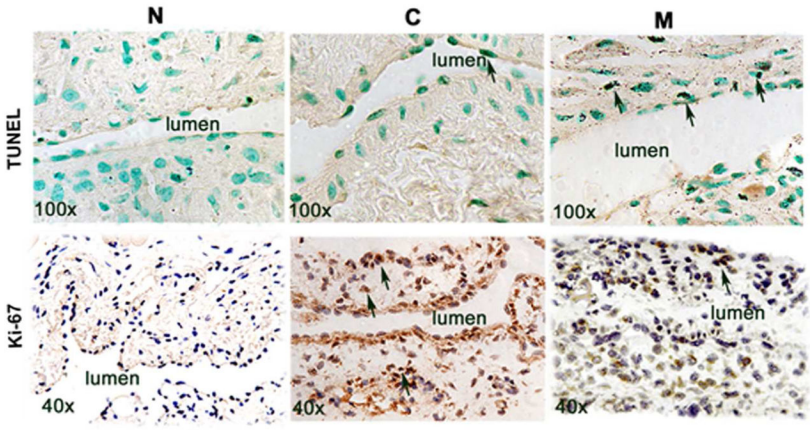

Figure 4.

TdT-mediated dNTP nick end labeling (TUNEL) and Ki-67 staining in murine AVF at day 7 and 21 after placement of AVF in outflow vein alone (**C**) and MSC transplanted vessels (**M**). **Upper panel** is the representative sections from TUNEL staining at outflow vein of the **M** transplanted and **C** vessels at day 7. Brown staining nuclei are positive for TUNEL (arrow). Negative control is shown where the recombinant terminal deoxynucleotidyl transferase enzyme was omitted. **Lower panel** is representative sections after Ki-67 staining in outflow vessels removed mesenchymal stem cell transplanted vessels (**M**) or arteriovenous fistula alone (**C**) at day 7 after AVF placement. Brown staining nuclei are positive for Ki-67. IgG negative controls are shown.

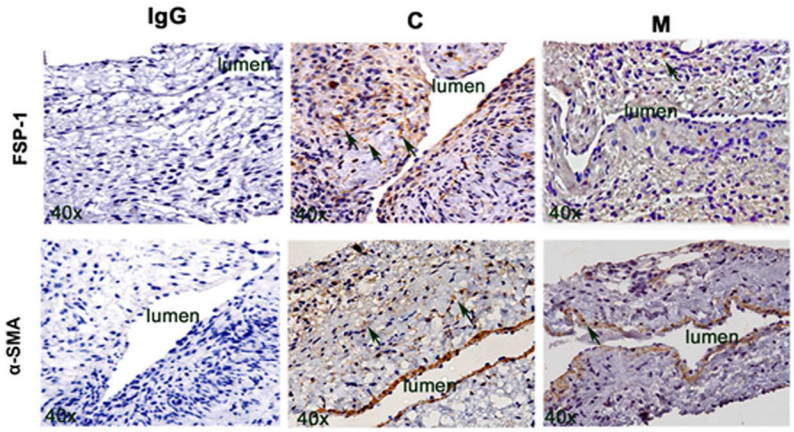

Figure 5.

FSP-1 and α-SMA staining in murine AVF at day 7 and 21 after placement of AVF in outflow vein alone (**C**) and MSC transplanted vessels (**M**). **Upper panel** is the representative sections after FSP-1 staining in the venous stenosis of the **M** transplanted and **C** vessels at day 21. Brown staining cells are positive for FSP-1 (arrow). IgG negative controls are shown. All are original magnification X 40. **Lower panel** is the representative sections after α-SMA staining in the venous stenosis of the **M** transplanted and **C** vessels at day 21. Brown staining cells are positive for α-SMA (arrow).

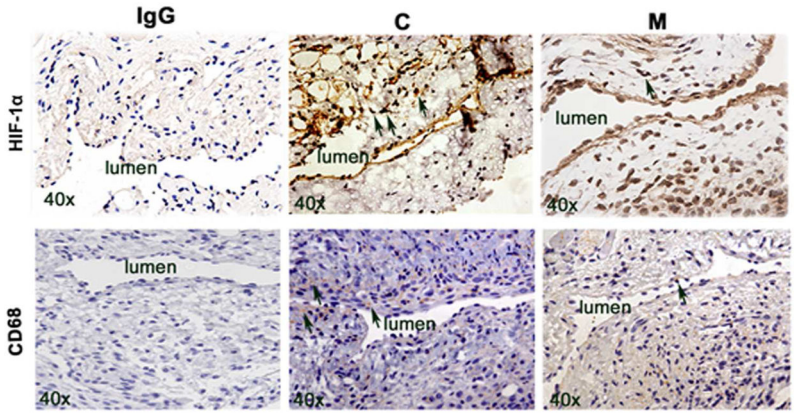

Figure 6.

HIF-1α and CD68 staining in murine AVF at day 7 and 21 after placement in outflow vein alone (**C**) and MSC transplanted vessels (**M**). **Upper panel** is the representative sections after HIF-1α staining in the venous stenosis of the **M** transplanted and **C** vessels at day 7. Brown staining nuclei are positive for HIF-1α staining. IgG negative controls are shown. All are original magnification X 40. **Lower panel** is the representative sections after CD68 staining in the venous stenosis of the **M** transplanted and **C** vessels at day 7. Brown staining cells are positive for CD68 staining.

Table 1

Mouse primers used

Gene	Sequence
Mcp-1	5′ – GGAGAGCTACAAGAGGATCAC – 3′ (sense) 5′ – TGATCTCATTTGGTTCCGATCC– 3′ (antisense)
18S	5′ – GTTCCGACCATAAACGATGCC-3′ (sense) 5′- TGGTGGTGCCCTTCCGTCAAT- 3′ (antisense)